Electronic Supplementary Material (ESI) for Journal of Materials Chemistry A.
This journal is © The Royal Society of Chemistry 2023

Supplementary Information

Boosting Oxygen Reduction Reaction using High Surface Area Graphitic-N Dominant Nitrogen Doped Carbon

Rizwan Haider[1], Shenqi Ding[1], Wenrui Wei[1], Yi Wan[1], Yu Huang[1], Renhuan Li[2,*], Liang Wu[1], Ayaz Muzammil[1], Yi Fan[2], Xianxia Yuan[1,*]

1 School of Chemistry and Chemical Engineering, Shanghai Jiao Tong University, Shanghai, 200240, P.R. China

2 Transportation College, Nanning University, Nanning, 530200, P.R. China

[*] **Corresponding authors:**

Renhuan Li, lirenhuan@nnxy.edu.cn

Xianxia Yuan, yuanxx@sjtu.edu.cn

Supplementary Equations

The reported potentials against RHE (E_{RHE}) in this work were calculated with equation (S1)

$$E_{RHE} = E°_{SCE} + 0.0591·pH + E_{SCE} \quad (S1)$$

where $E°_{SCE}$ is the standard electrode potential for SCE and E_{SCE} is the recorded potential against SCE.

The electron transfer number during ORR was obtained from RDE data at various electrode rotation speeds with equations (S2)-(S4),

$$\frac{1}{I}=\frac{1}{I_k}+\frac{1}{I_d}=\frac{1}{I_k}+\frac{1}{B\omega^{1/2}} \quad (S2)$$

$$\frac{1}{I}=\frac{1}{I_k}+\frac{1}{0.62D_o^{2/3}\upsilon^{-1/6}nFC_o\omega^{1/2}} \quad (S3)$$

$$B=0.62D_o^{2/3}\upsilon^{-1/6}nFAC_o \quad (S4)$$

where I, I_k and I_d are the current density, kinetic current density and diffusion limiting current density, respectively, F is Faraday constant (96485 C mol^{-1}), A is the electrode area (0.1963 cm^2 in this work), C_o is the oxygen concentration in 0.1 M KOH (1.22× 10^{-6} mol cm^{-3}), D_o is the diffusion coefficient of O_2 in electrolyte (1.9×10^{-5} cm^2 s^{-1}), υ is the kinematic viscosity (0.0113 cm^2 s^{-1}) in 0.1 M KOH, and ω is the angular frequency of electrode rotation (rad s^{-1}). According to these equations, the K-L plot of inverse current vs inverse square root of the electrode rotation rate yields a straight line and its slope could be used to give the charge transfer number (n).

Kinetic current density (J_K) was calculated with equation (S5),

$$J_K=\frac{J_L \times J_{0.80}}{J_L - J_{0.80}} \quad (S5)$$

where J_L is the limiting current density (mA cm^{-2}) at 0.45 V, and $J_{0.80}$ stands for the current density (mA cm^{-2}) at 0.80 V in LSV curves recorded at 1600 rpm.

The calculation of electron transfer number (n) and percentage yield of hydrogen peroxide (H_2O_2%) during ORR from RRDE data were carried out by using equation (S6) and (S7), respectively.

$$n = 4 \times \frac{i_d}{i_d+(i_r/N)} \quad (S6)$$

$$H_2O_2\% = 200 \times \frac{i_r/N}{i_d+(i_r/N)} \quad (S7)$$

where i_d is the disk current, i_r is the ring current and N is collection efficiency of ring electrode (which is 0.37 as provided by the supplier).

The dissociative mechanism for ORR

$$O_2 + * \rightarrow *O_2 \quad \text{(S8)}$$

$$*O_2 \rightarrow *O + *O \quad \text{(S9)}$$

$$*O + *O + H_2O \rightarrow *O + *OH + OH^- \quad \text{(S10)}$$

$$*O + *OH + H_2O \rightarrow *OH + *OH + OH^- \quad \text{(S11)}$$

$$*OH + *OH + e^- \rightarrow *OH + OH^- \quad \text{(S12)}$$

$$*OH + e^- \rightarrow OH^- + * \quad \text{(S13)}$$

The associative mechanism for ORR

$$O_2 + * \rightarrow *O_2 \quad \text{(S14)}$$

$$*O_2 + H_2O + e^- \rightarrow *OOH + OH^- \quad \text{(S15)}$$

$$*OOH + e^- \rightarrow *O + OH^- \quad \text{(S16)}$$

$$*O + H_2O + e^- \rightarrow *OH + OH^- \quad \text{(S17)}$$

$$*OH + e^- \rightarrow OH^- + * \quad \text{(S18)}$$

Supplementary Figures

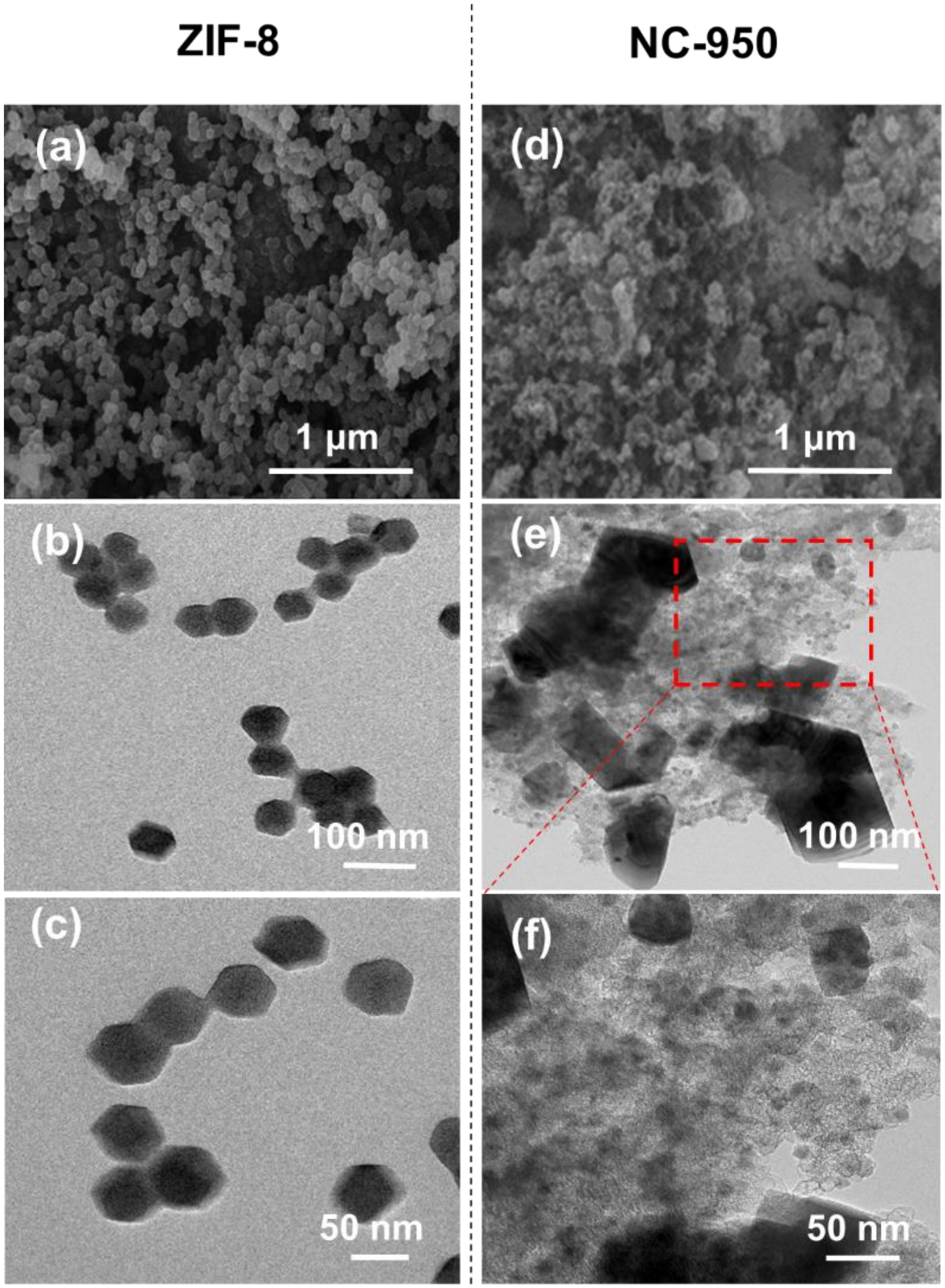

Figure S1. SEM of (a) ZIF-8 and (d) NC-950. TEM of (b,c) ZIF-8 and (e,f) NC-950.

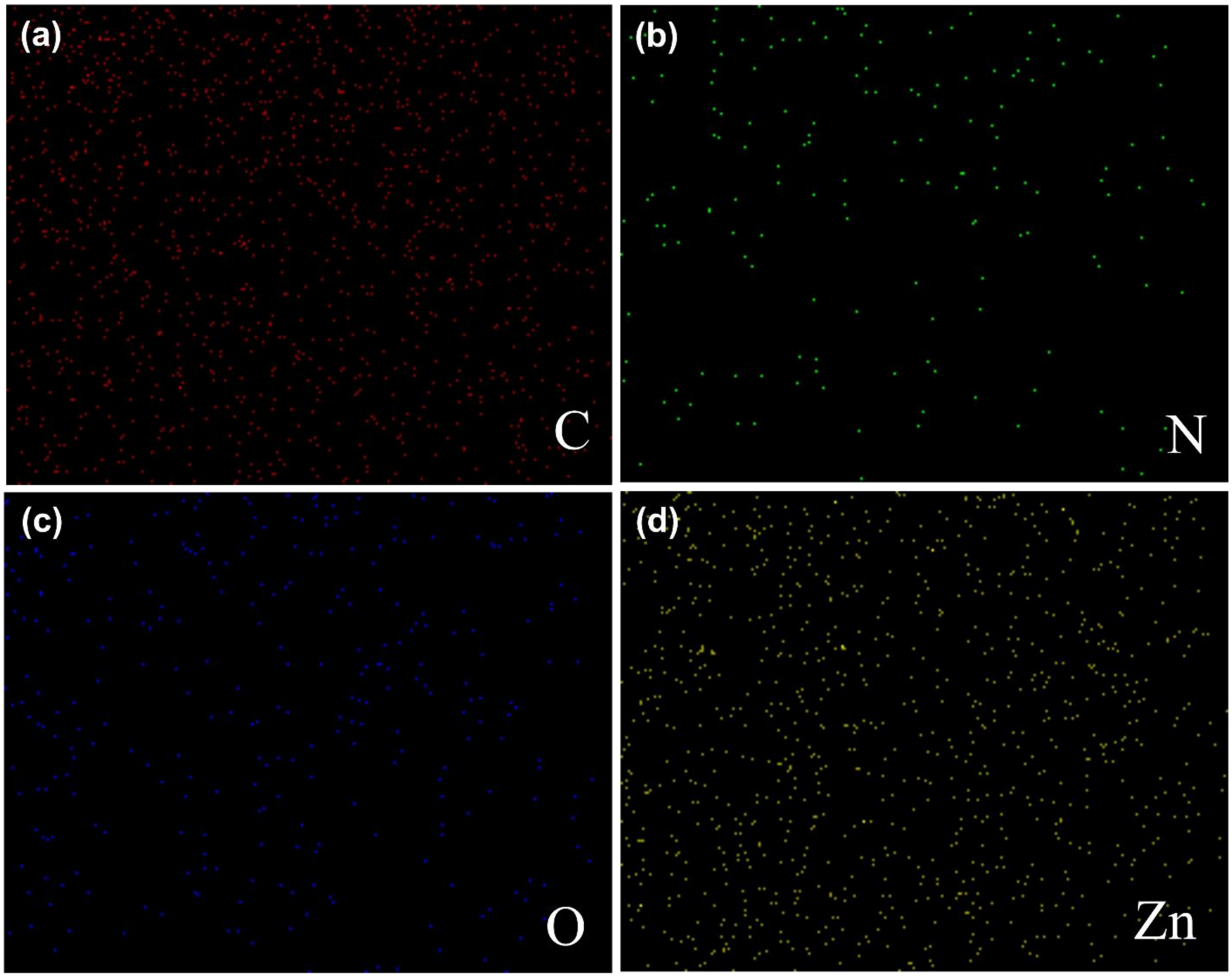

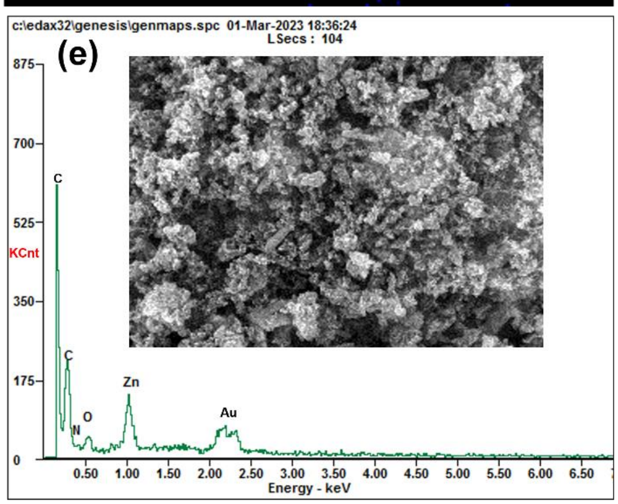

(f)

Element	Wt%	At%
CK	45.91	66.14
NK	12.32	15.22
OK	9.28	10.04
ZnL	32.49	8.60
Matrix	Correction	ZAF

Figure S2. EDS mapping presenting (a) C, (b) N, (c) O and (d) Zn in NC-950. (e) EDS spectra with the image as inset and (f) Wt.% and At.% of C, N, O and Zn in NC-950.

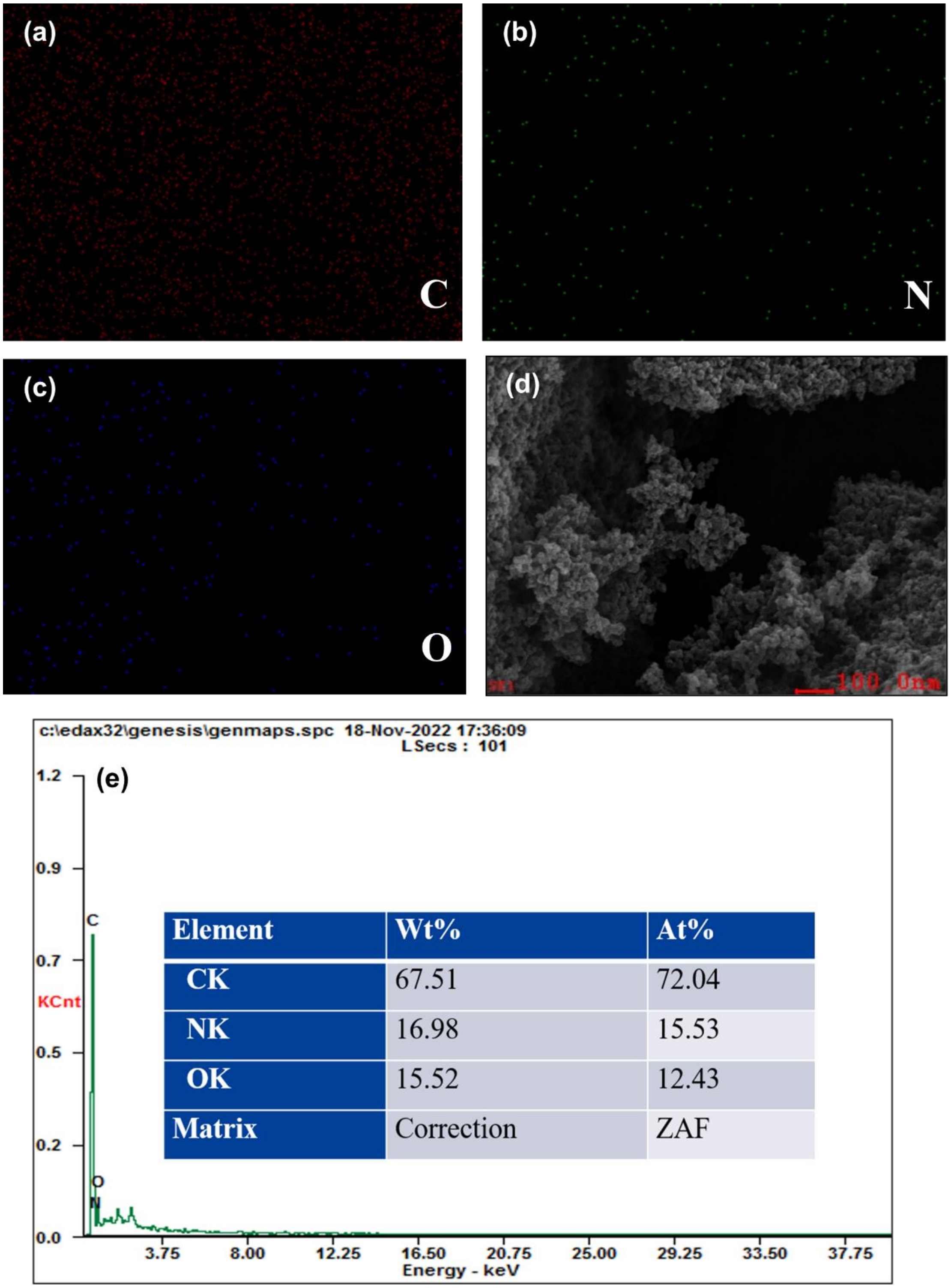

Element	Wt%	At%
CK	67.51	72.04
NK	16.98	15.53
OK	15.52	12.43
Matrix	Correction	ZAF

Figure S3. EDS mapping presenting (a) C, (b) N, and (c) O in NC-1000. (d) EDS image and (e) the spectra along with Wt.% and At.% of C, N and O in NC-1000.

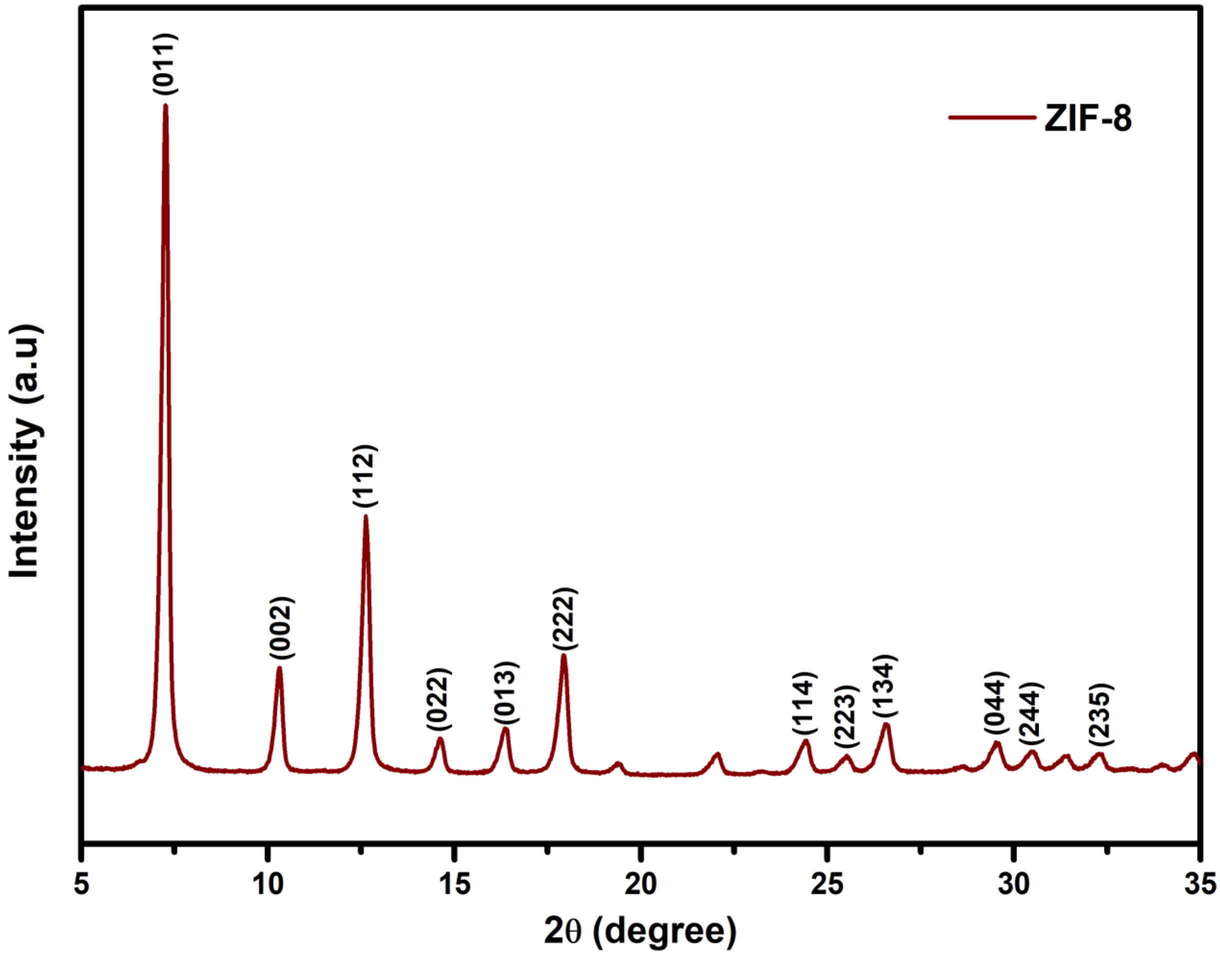

Figure S4. XRD pattern of ZIF-8.

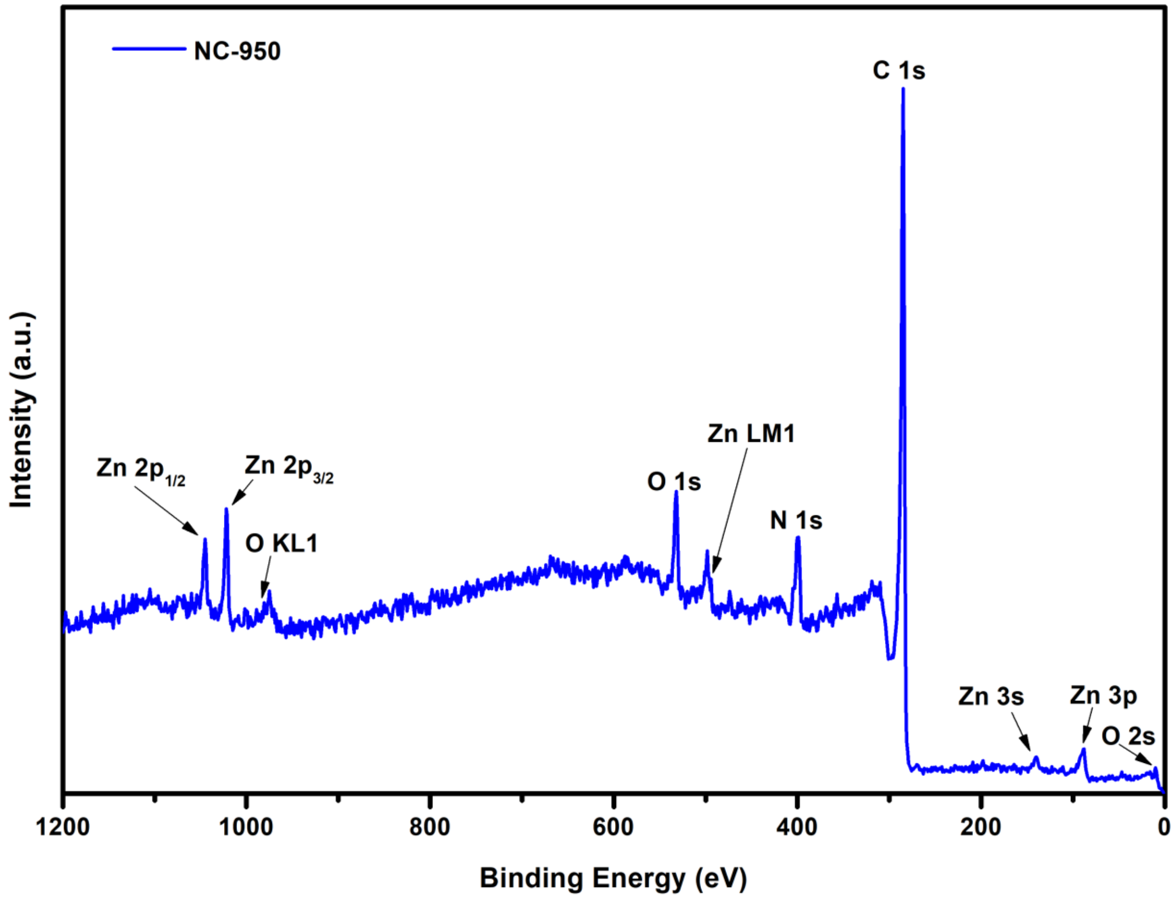

Figure S5. XPS survey spectrum of NC-950.

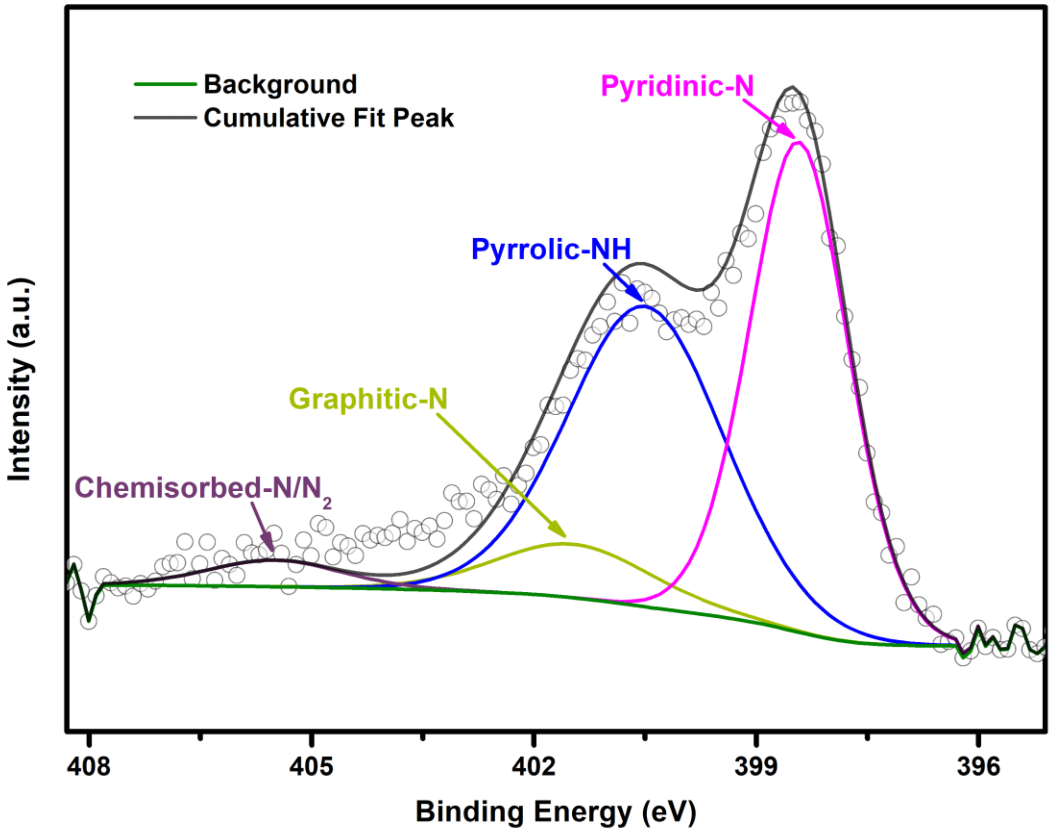

Figure S6. Deconvoluted N 1s spectra of NC-950.

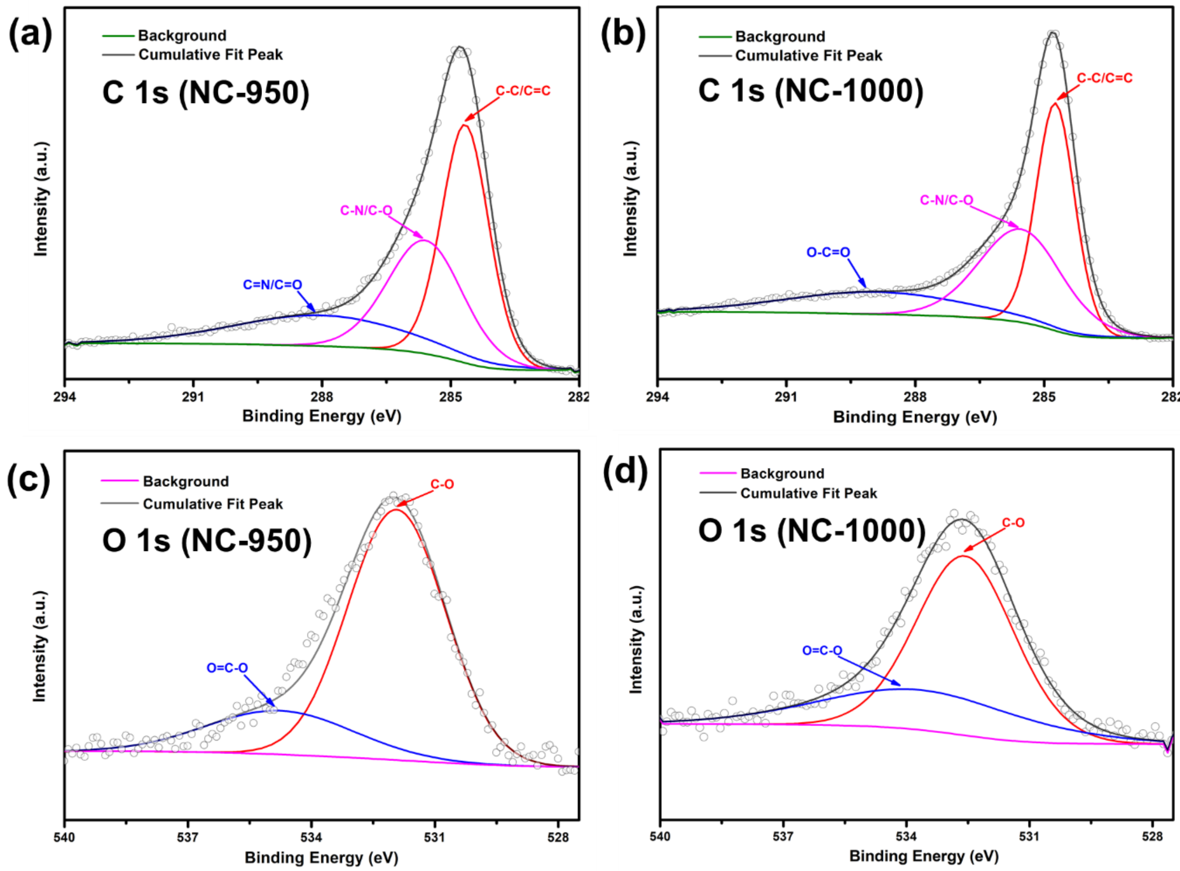

Figure S7. Deconvoluted XPS spectra of (a,b) C 1s and (c,d) O 1s for NC-950 (a, c) and NC-1000 (b, d).

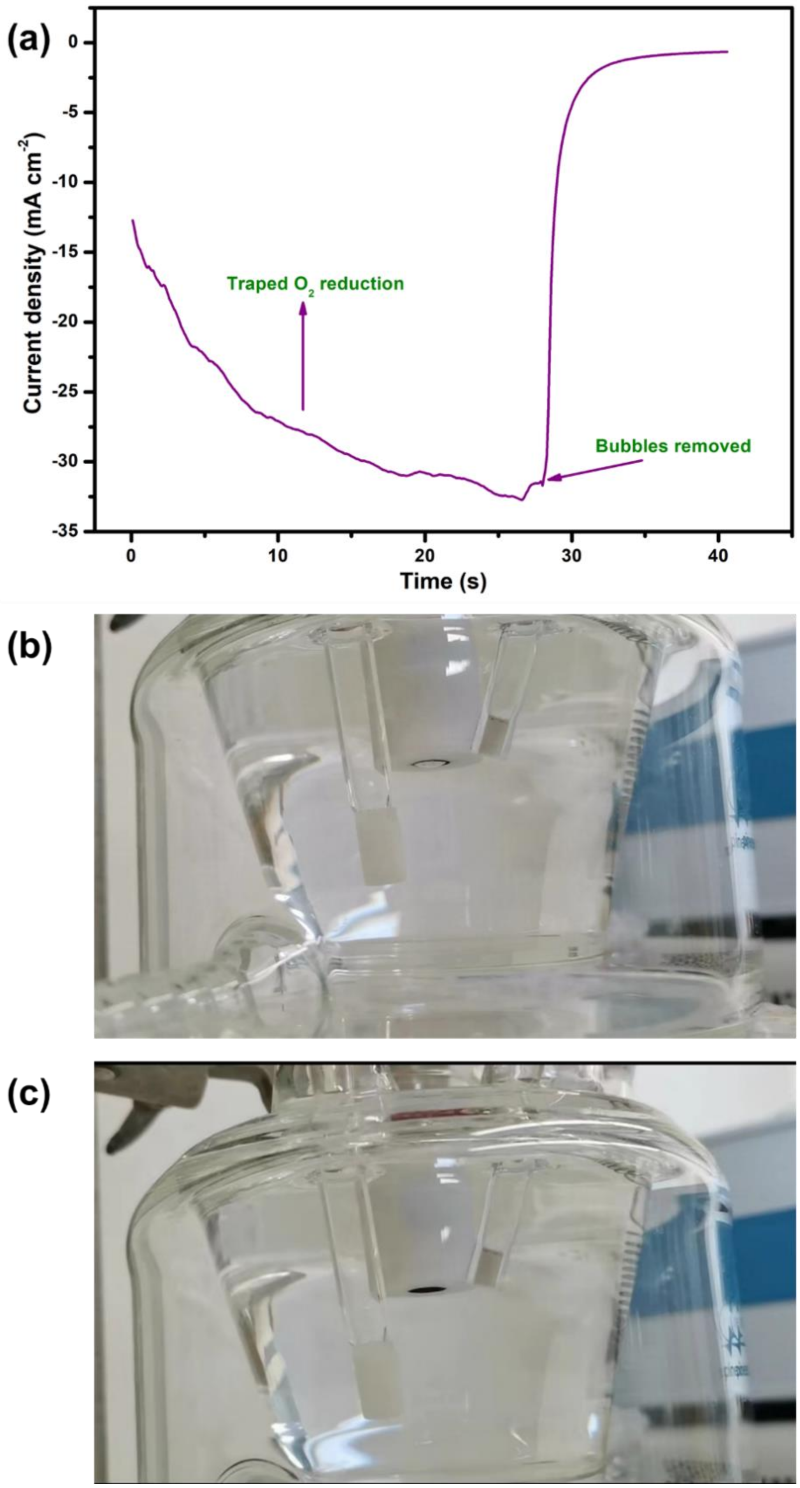

Figure S8. (a) The trapped O_2 reduction current density vs. time during the bubble removal treatment by applying a high reducing voltage of 0.37 V, and a visual representation of the electrode surface (a) before and (b) after the bubble removal experiment.

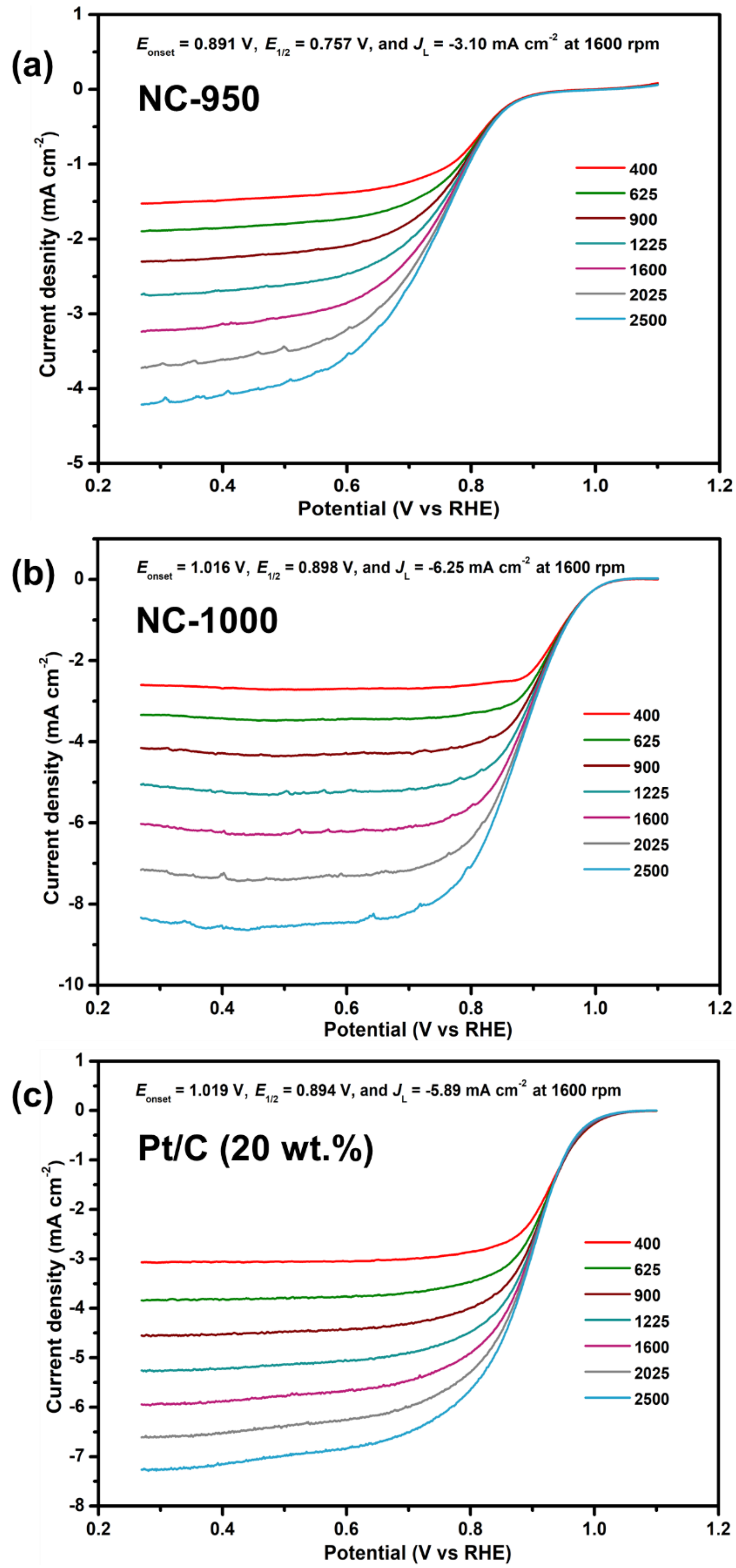

Figure S9. LSV curves of (a) NC-950, (b) NC-1000 and (c) Pt/C (20 wt.%) recorded in O_2 saturated 0.1 M KOH solution at electrode rotating rates of 400-2500 rpm.

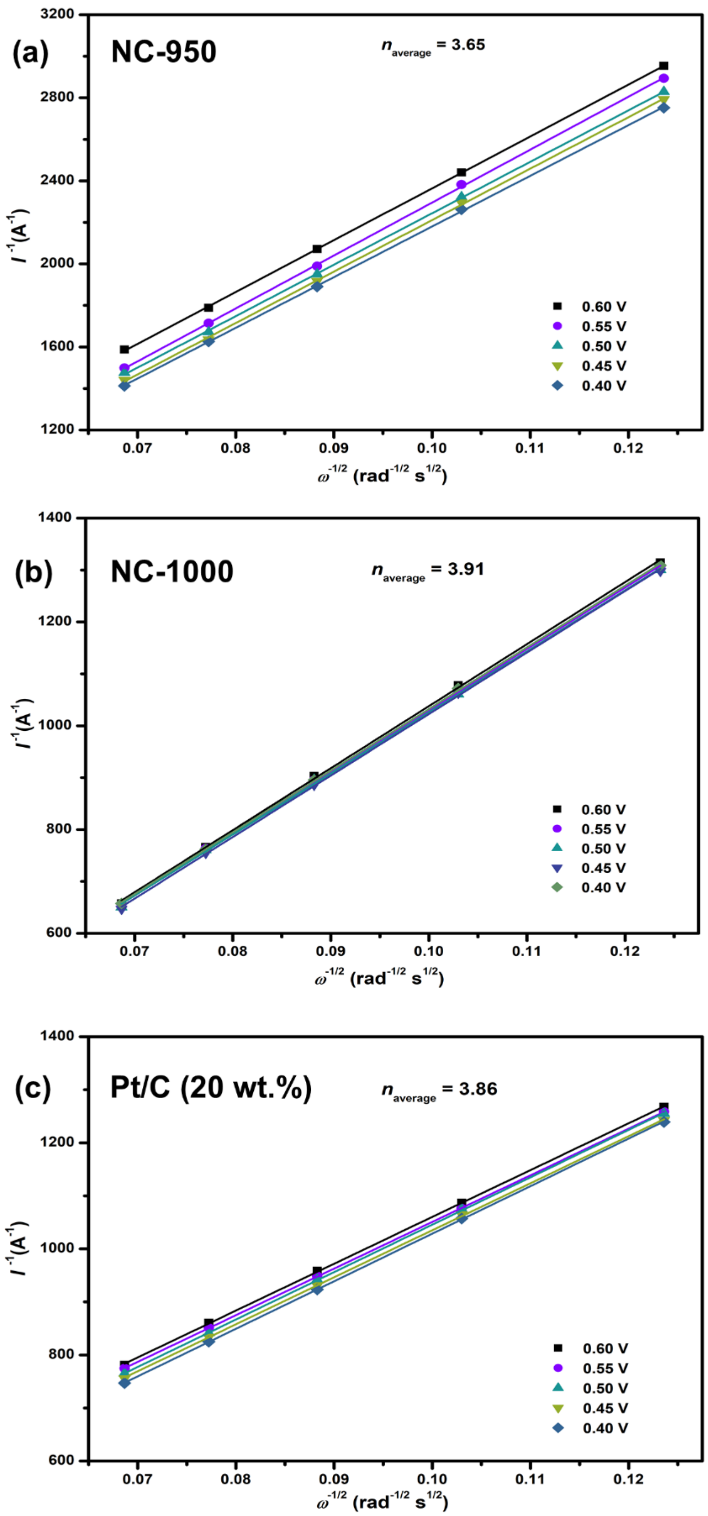

Figure S10. K-L plots derived from the LSV curves in Fig. S8 for (a) NC-950, (b) NC-1000 and (c) Pt/C (20 wt.%) at 625 to 2025 rpm.

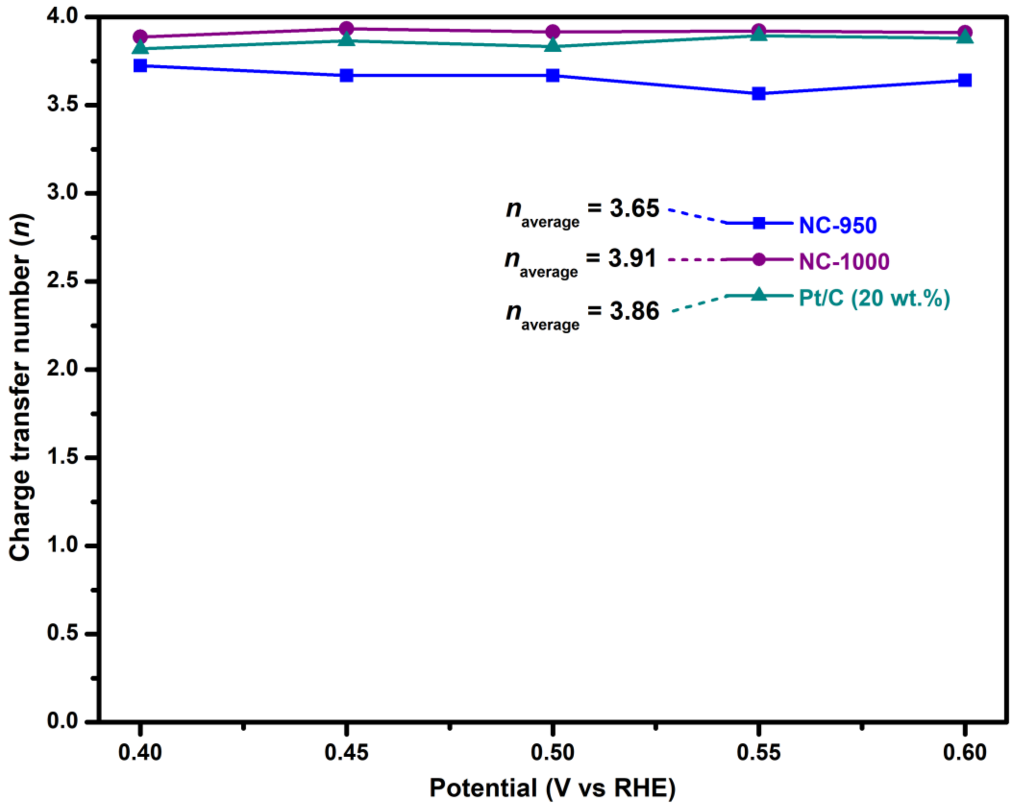

Figure S11. Potential dependence of the charge transfer number calculated from the K-L plots in Fig. S10 for NC-950, NC-1000 and Pt/C (20 wt.%).

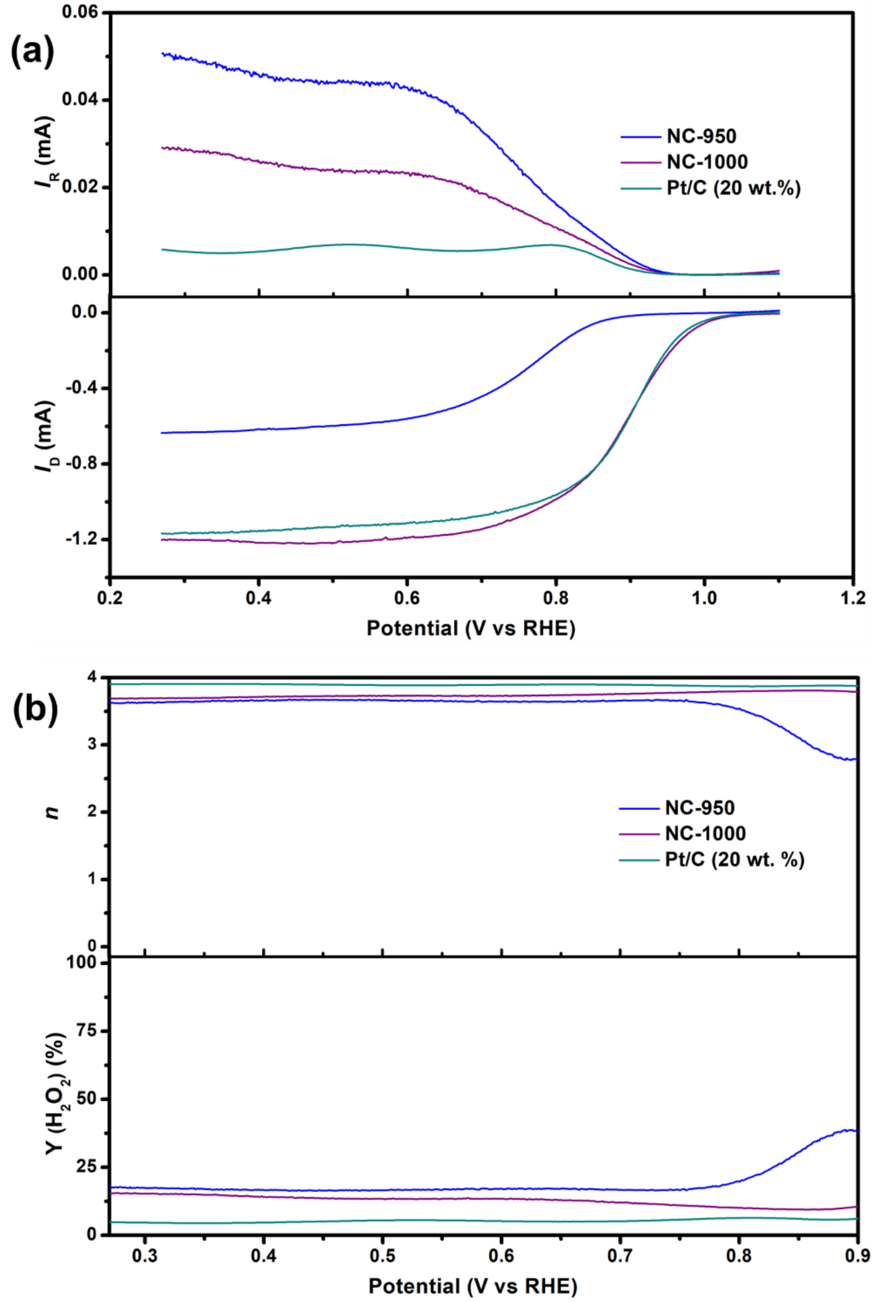

Figure S12. (a) RRDE data and the (b) calculated charge transfer number (*n*) and H_2O_2 (%) yield for NC-950, NC-1000 and Pt/C (20 wt.%).

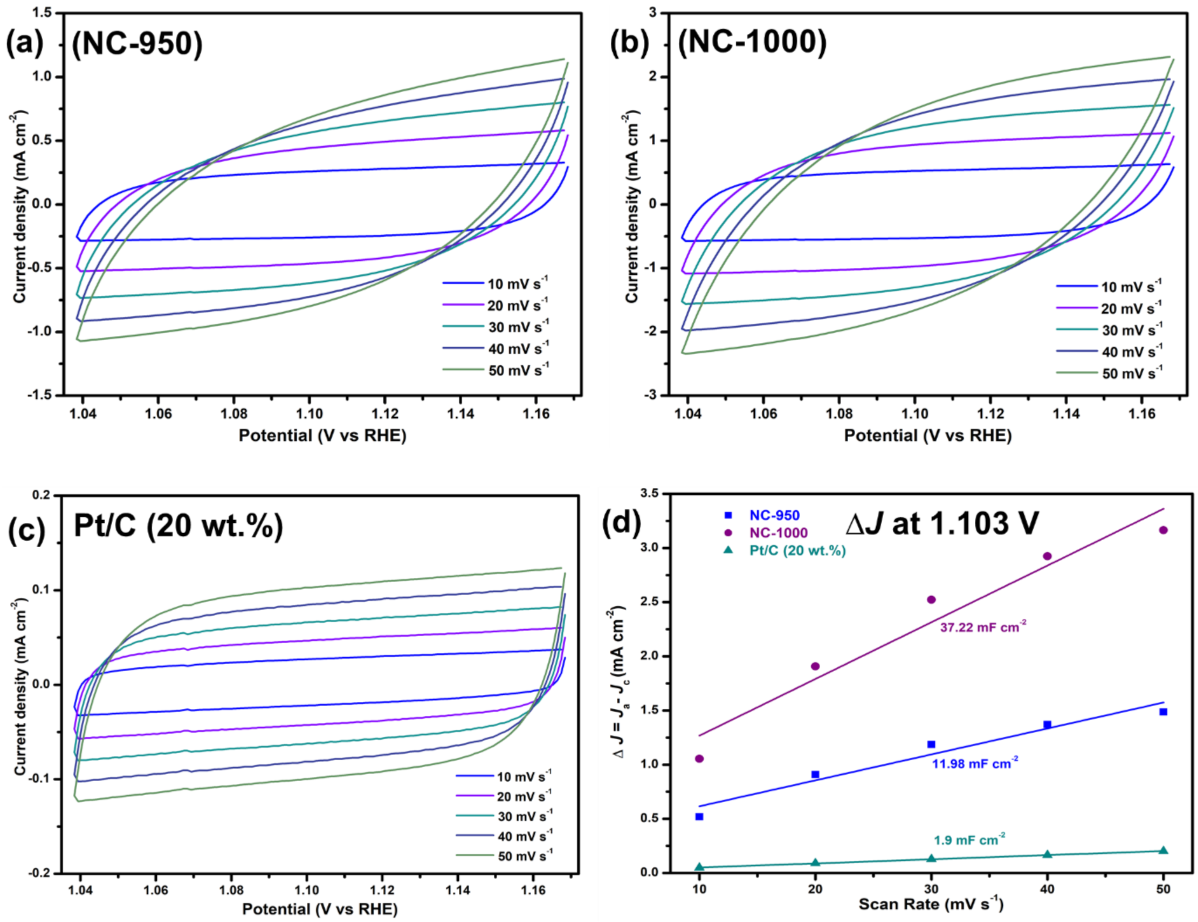

Figure S13. CV curves in the non-Faradic region for (a) NC-950, (b) NC-1000 and (c) Pt/C (20 wt.%) at various scan rates. (d) Line fitted plots of scan rate vs ΔJ at 1.103 V for the estimation of double layer capacitance (C_{dl}).

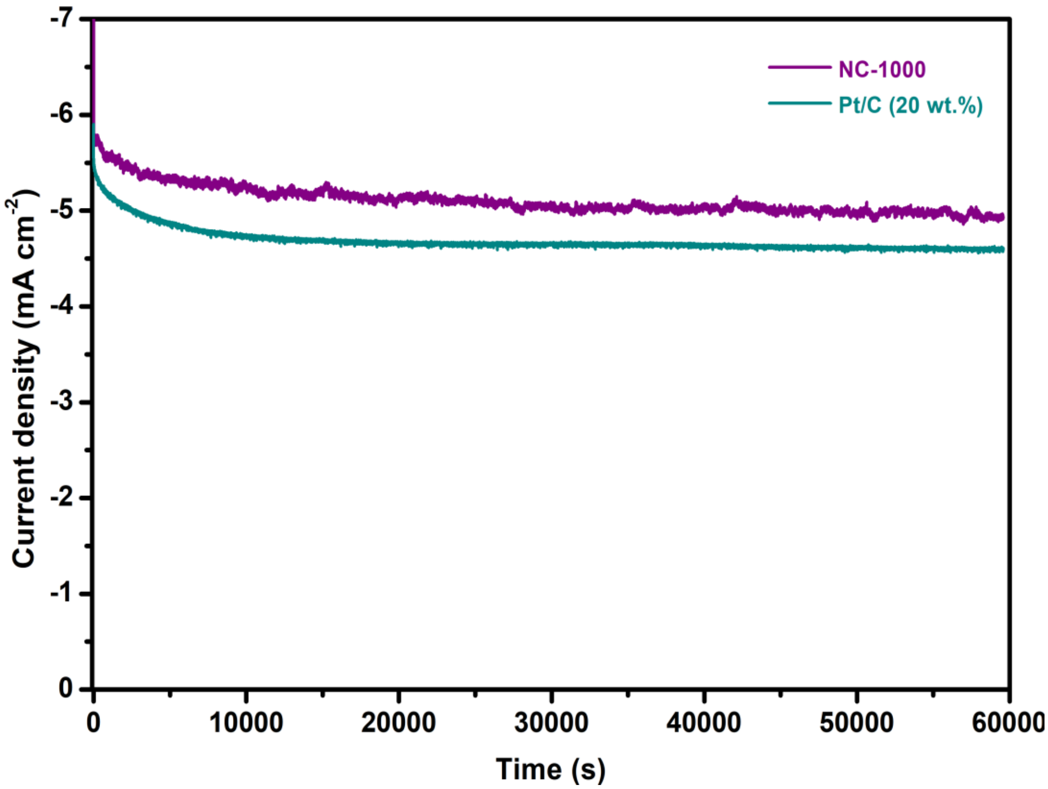

Figure S14. Chronoamperometric current density of NC-1000 and Pt/C (20 wt.%) after 60000 s operation at 0.6 V with 1600 rpm in O_2 saturated 0.1 M KOH solution.

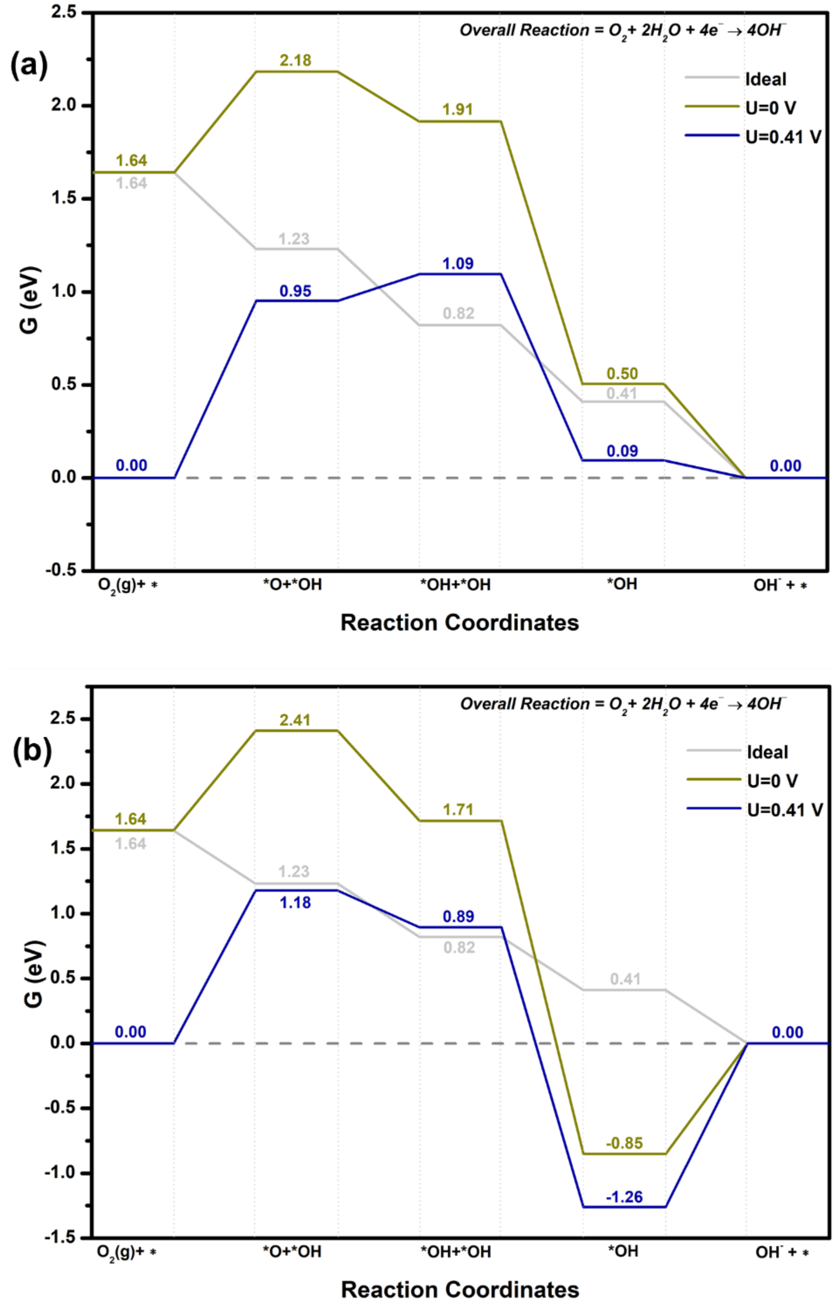

Figure S15. Gibbs free energy for various reaction intermediates following dissociative ORR mechanism in alkaline electrolyte on (a) graphitic N sites and (b) pyridinic-N sites present in NC-1000.

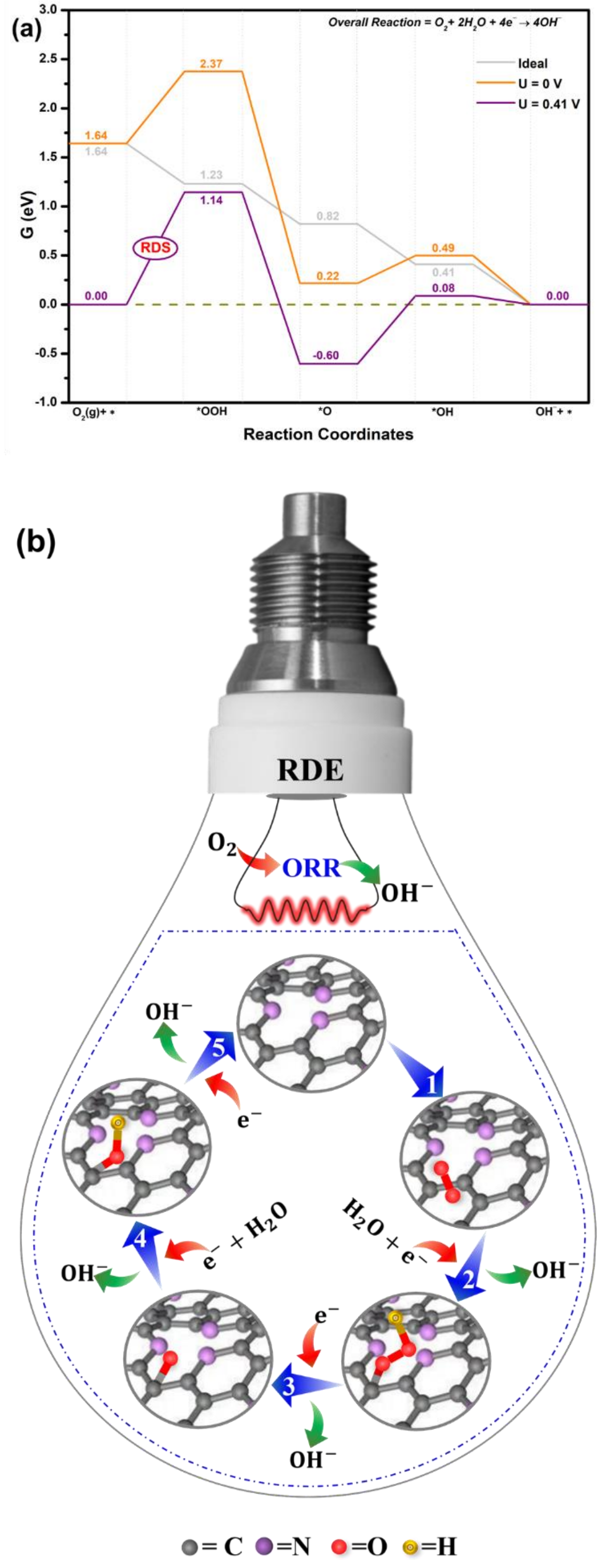

Figure S16. (a) Gibbs free energy for various reaction intermediates following associative ORR mechanism in alkaline electrolyte and (b) the proposed ORR mechanism on pyridinic-N sites present in NC-1000.

Table S1. ORR performance comparison of NC-1000 with recently reported nitrogen doped carbon catalysts in 0.1 M KOH solution except for Ref. 15, where 1 M KOH was used. All the voltages are mentioned against RHE.

Journal name (Publication year)	Material Name	E_{Onset} (V)	$E_{1/2}$ (V)	J_L (mA cm^{-2})	Tafel slope (mV dec^{-1})	Stability	Durability ($E_{1/2}$ loss)	Ref.
This work	NC-1000	1.016	0.898	6.25	38.5	85.74 % at 0.6V (60000 s)	26 mV (5000 cycles)	
ChemElectroChem (2019)	100N8/HTC	0.90	0.81	3.90	65	100 % at 0.81 V (3600 s)	----	1
Catal. Today (2019)	CS-HPCNS-1000-5	0.99	0.79	3.75	----	87 % at 0.77 V (12000 s)	----	2
Appl. Catal. B. (2019)	nitrogen-doped graphene	0.96	0.83	4.90	60	----	No loss (5000 cycles)	3
Chem. Eng. J. (2022)	h-N-CFs-800	1.01	0.87	5.86	79.3	93.4 % at 0.7 V (6000 s)	14 mV (5000 cycles)	4
Chem. Eng. J. (2022)	PNC-30	1.00	0.90	6.10	57	96 % at 0.4 V (60000 s)	----	5
J. Colloid Interface Sci. (2020)	PS-900	1.00	0.85	5.84	68	100 % at 0.67 V (50000 s)	----	6
Chem. Eur. J. (2020)	2DPCs-a	0.93	0.83	5.30	64	80.2%, at 0.75 V (35000 s)	----	7
Nat. Commun. (2018)	N-HsGDY-900	1.02	0.85	6.20	64.4	100 % at 0.7 V (36000 s)	Negligible loss (5000 cycles)	8
ACS Omega (2020)	AWC-1	0.92	0.85	5.00	55.6	----	No loss (5000 cycles)	9
Nanoscale Res. Lett. (2019)	Me-CFZ-900	0.99	0.86	5.10	----	----	21 mV (5000 cycles)	10
J. Colloid Interface Sci. (2022)	CMP-NP-900	0.93	0.86	4.45	----	89.6 % at 0.7 V (10000 s)	Negligible loss (3000 cycles)	11
J. Adv. Ceram. (2021)	NPC-1000	0.925	0.86	4.90	64.9	78 % at 0.65 V (28800 s)	----	12
Carbon (2023)	D-NCNS	1.05	0.873	5.65	98.2	----	18 mV (12000 cycles)	13

Energy Environ. Sci. (2019)	NCN-1000-5	0.95	0.82	6.43	86	85.6 % at 0.67 V (12000 s)	----	[14]
Sci. Adv. (2016)	N-GRW	0.92	0.84	3.50	53	90 % at 0.7 V (43200 s)	15 mV (2000 cycles)	[15]
Carbon (2020)	N-hG	0.91	0.833	5.25	78	90.7 % at 0.6 V (10000 s)	----	[16]
Angew Chem (2019)	PD-C	0.911	0.833	4.80	----	96 % at 0.67 V (10000 s)	----	[17]
Adv. Funct. Mater. (2021)	NCF	1.00	0.85	6.00	71	88.9 % at 0.7 V (86400 s)	----	[18]
Appl. Catal. B. (2020)	N-CNT-3 h	0.95	0.83	5.70	89	----	13 mV (10000 cycles)	[19]

References

1. A. Wütscher, T. Eckhard, D. Hiltrop, K. Lotz, W. Schuhmann, C. Andronescu and M. Muhler, *ChemElectroChem*, 2019, **6**, 514-521.
2. P. Cao, Y. Liu, X. Quan, J. Zhao, S. Chen and H. Yu, *Catalysis Today*, 2019, **327**, 366-373.
3. N. Komba, Q. Wei, G. Zhang, F. Rosei and S. Sun, *Applied Catalysis B: Environmental*, 2019, **243**, 373-380.
4. S. Li, Y. Wang, Y. Ding, Y. He, Y. Zhang, S. Li, J. Zhang and Y. Chen, *Chemical Engineering Journal*, 2022, **430**, 132969.
5. B. Liu, F. Liu, D. Lu, S. Zhang, C. Zhang, Z. Gao, L. Shi, Y. Liu, J. X. Shi and L. Zhang, *Chemical Engineering Journal*, 2022, **430**, 132762.
6. L. Yu, C. Yang, W. Zhang, W. Liu, H. Wang, J. Qi and L. Xu, *Journal of Colloid and Interface Science*, 2020, **575**, 406-415.
7. K. Tu, L. Zou, C. Yang, Y. Su, C. Lu, J. Zhu, F. Zhang, C. Ke and X. Zhuang, *Chemistry–A European Journal*, 2020, **26**, 6525-6534.
8. Q. Lv, W. Si, J. He, L. Sun, C. Zhang, N. Wang, Z. Yang, X. Li, X. Wang and W. Deng, *Nature Communications*, 2018, **9**, 3376.
9. K. t. Kaare, E. Yu, A. Volperts, G. Dobele, A. Zhurinsh, A. Dyck, G. Niaura, L. Tamasauskaite-Tamasiunaite, E. Norkus and M. Andrulevičius, *ACS Omega*, 2020, **5**, 23578-23587.
10. C. Guo, Y. Li, Y. Xu, Q. Xiang, L. Sun, W. Zhang, W. Li, Y. Si and Z. Luo, *Nanoscale Research Letters*, 2019, **14**, 1-11.
11. H. Sun, P. Zhou, X. Ye, J. Wang, Z. Tian, Z. Zhu, C. Ma, W. Liang and A. Li, *Journal of Colloid and Interface Science*, 2022, **617**, 11-19.
12. Z. Mo, W. Yang, S. Gao, J. K. Shang, Y. Ding, W. Sun and Q. Li, *Journal of Advanced Ceramics*, 2021, **10**, 714-728.
13. H. Gao, S. Wang, W.-C. M. Cheong, K. Wang, H. Xu, A. Huang, J. Ma, J. Li, W.-F. A. Ip and K. San Hui, *Carbon*, 2023, **203**, 76-87.
14. H. Jiang, J. Gu, X. Zheng, M. Liu, X. Qiu, L. Wang, W. Li, Z. Chen, X. Ji and J. Li, *Energy & Environmental Science*, 2019, **12**, 322-333.
15. H. B. Yang, J. Miao, S.-F. Hung, J. Chen, H. B. Tao, X. Wang, L. Zhang, R. Chen, J. Gao and H. M. Chen, *Science Advances*, 2016, **2**, e1501122.
16. Y. Bian, H. Wang, J. Hu, B. Liu, D. Liu and L. Dai, *Carbon*, 2020, **162**, 66-73.
17. J. Zhu, Y. Huang, W. Mei, C. Zhao, C. Zhang, J. Zhang, I. S. Amiinu and S. Mu, *Angewandte Chemie International Edition*, 2019, **58**, 3859-3864.
18. L. Zhang, T. Gu, K. Lu, L. Zhou, D. S. Li and R. Wang, *Advanced Functional Materials*, 2021, **31**, 2103187.
19. S. Yi, X. Qin, C. Liang, J. Li, R. Rajagopalan, Z. Zhang, J. Song, Y. Tang, F. Cheng and H. Wang, *Applied Catalysis B: Environmental*, 2020, **264**, 118537.